

FTIR spectroscopy can predict organic matter quality in regenerating cutover peatlands.

Rebekka R.E. Artz, Stephen J. Chapman, A.H. Jean Robertson, Jacqueline M. Potts, Fatima Laggoun-Défarge, Sébastien Gogo, Laure Comont, Jean-Robert Disnar, Andre-Jean Francez

► **To cite this version:**

Rebekka R.E. Artz, Stephen J. Chapman, A.H. Jean Robertson, Jacqueline M. Potts, Fatima Laggoun-Défarge, et al.. FTIR spectroscopy can predict organic matter quality in regenerating cutover peatlands.. Soil Biology and Biochemistry, Elsevier, 2008, 40 (2), pp.515-527. insu-00173352

HAL Id: insu-00173352

<https://hal-insu.archives-ouvertes.fr/insu-00173352>

Submitted on 19 Sep 2007

HAL is a multi-disciplinary open access archive for the deposit and dissemination of scientific research documents, whether they are published or not. The documents may come from teaching and research institutions in France or abroad, or from public or private research centers.

L'archive ouverte pluridisciplinaire **HAL**, est destinée au dépôt et à la diffusion de documents scientifiques de niveau recherche, publiés ou non, émanant des établissements d'enseignement et de recherche français ou étrangers, des laboratoires publics ou privés.

1

2 **FTIR spectroscopy can predict organic matter quality in**
3 **regenerating cutover peatlands**

4 (Running title: Whole soil FTIR on peat)

5

6 Rebekka R.E. Artz¹, Stephen J. Chapman¹, A.H. Jean Robertson¹, Jacqueline M.
7 Potts², Fatima Laggoun-Défarge³, Sébastien Gogo³, Laure Comont³, Jean-Robert
8 Disnar³ and Andre-Jean Francez⁴

9

10 ¹ *Soils Group, The Macaulay Institute, Craigiebuckler, Aberdeen, AB15 8QH, UK.*

11 ² *Biomathematics and Statistics Scotland (BioSS), The Macaulay Institute,*
12 *Craigiebuckler, Aberdeen AB15 8QH, UK.*

13 ³ *Institut des Sciences de la Terre d'Orléans (ISTO), UMR 6113 CNRS/Université*
14 *d'Orléans, Bt Géosciences, Rue de St Amand, BP 6759, 45067 Orléans cedex 2,*
15 *France.*

16 ⁴ *Interactions biologiques et transferts de matières, UMR CNRS 6553 Ecobio,*
17 *Université de Rennes 1, 35042 Rennes cedex, France.*

18

19 Date of receipt:

20 *Keywords: Fourier-Transform Infrared Spectroscopy, peat, organic matter quality,*
21 *carbohydrates, C:N ratio, organic micro-remains*

22

23

24 *Corresponding author: Rebekka R.E.Artz, The Macaulay Institute, fax: (+44) (0)1224*

25 *498207; e-mail: r.artz@macaulay.ac.uk*

26 **Abstract**

27 **Vegetational changes during the restoration of cutover peatlands leave a legacy**
28 **in terms of the organic matter quality of the newly formed peat. Current efforts**
29 **to restore peatlands at a large scale therefore require low cost, and high**
30 **throughout, techniques to monitor the evolution of organic matter. In this study,**
31 **we assessed the Fourier Transform Infrared (FTIR) spectra of the organic**
32 **matter in peat samples at various stages of peatland regeneration from five**
33 **European countries. Using predictive partial least squares analyses, we were able**
34 **to reconstruct both peat C:N ratio and carbohydrate signatures, but not the**
35 **micromorphological composition of vegetation remains, from the FTIR datasets.**
36 **Despite utilising different size fractions, both carbohydrate (< 200 µm fraction)**
37 **and FTIR (bulk soil) analyses report on the composition of plant cell wall**
38 **constituents in the peat and therefore essentially reveal the composition of the**
39 **parent vegetational material. This suggests that FTIR analysis of peat may be**
40 **used successfully for evaluation of the present and future organic matter**
41 **composition of peat in monitoring of restoration efforts.**

42

43 **1. Introduction**

44 Northern Peatlands are composed almost entirely of decomposing plant
45 material and store approximately a third of all soil organic matter (Gorham, 1991)
46 even though their total cover only extends to 3-5 % of the global land area. Peat
47 extraction for fuel and horticultural use has steadily diminished this carbon stock,
48 with the largest quantities of peat having been extracted in the mid to late 20th century
49 (Chapman et al., 2003). Various restoration programs have since been designed to
50 encourage revegetation of cut-over peatlands (Gorham and Rochefort, 2003).
51 Although some of these programs have demonstrated that annual gaseous emissions

52 show a return to net carbon sequestration (Tuittila et al., 1999) or at least reduce net
53 emissions (Waddington and Warner, 2001), it is not known how peatland restoration
54 affects the pool of soil organic matter and hence the long-term regeneration of the
55 carbon sequestration potential. Increased losses of dissolved organic carbon (DOC)
56 have been observed from many peatland ecosystems in the past decades (Freeman et
57 al., 2001), and some of this can be ascribed to increased turnover of the soil organic
58 matter (Glatzel et al., 2003). Currently, monitoring efforts of the evolution of soil
59 organic matter quality during restoration of peatlands have only a limited array of
60 tools. Generally, bulk measures such as total and soluble organic carbon and nitrogen,
61 and their ratios, have been most often used to assess restoration success (Andersen et
62 al., 2006; Comont et al., 2006). Similarly, a technique often employed in peat organic
63 matter compositional studies is analysis of the patterns of carbohydrate monomers
64 derived from plant cellulose and hemicelluloses as these are indicative of the source
65 plant composition and the preservation status of these remains (Cheshire, 1979; Moers
66 et al., 1989, 1990; Bourdon et al., 2000). Comont et al., (2006) used peat C:N ratios
67 combined with micromorphological and carbohydrate composition of peat in a
68 pioneering study to elucidate the evolution of organic matter with regeneration. These
69 techniques, however, are expensive and time consuming processes. FTIR
70 spectroscopy is a commonly used technique capable of distinguishing the principal
71 chemical classes in soil organic matter, such as carbohydrates, lignins, cellulose, fats
72 and/or lipids and proteinaceous compounds, through the vibrational characteristics of
73 their structural chemical bonds. The use of attenuated total reflectance accessories, in
74 particular those utilising very hard crystals such as diamond, has further advanced the
75 use of FTIR in soils and other solid residues. Dilution with KBr is no longer
76 necessary, reproducibility is increased and the nondestructive nature of this analysis
77 allows the sample to be re-used for other analyses. FTIR spectroscopy has been used

78 successfully on whole soils to describe the status of decomposition in different
79 horizons (Haberhauer et al., 1998, 1999; Chapman et al., 2001), for example through
80 following the reduction of the carbohydrate markers with depth. Using multivariate
81 statistics, FTIR data can be used as quantitative indicators of the composition of the
82 soil organic matter to distinguish soil horizons (Haberhauer et al., 1999, 2000).
83 Models utilising partial least squares (PLS) analysis have been applied to FTIR data
84 to predict various chemical and physical qualities of organic materials, including
85 studies of the lignin and carbohydrate contents of wood and woody peat (Durig et al.,
86 1988; Tucker et al., 2001; Bjarnestad and Dahlman, 2002) and the phenolic and
87 carbohydrate contents of food (e.g. Coimbra et al., 2005). This study investigated the
88 potential use of FTIR spectroscopy data as indicators of peat organic matter quality in
89 regenerating peatlands. We determined various chemical and micromorphological
90 characteristics of peat samples from profiles at sites at different stages of regeneration
91 from five cutover European peatlands and tested the power of partial least squares
92 analysis using FTIR data to predict these organic matter characteristics. In large scale
93 restoration projects, it would be advantageous to be able to use low cost and high
94 throughput techniques in order to assess the success of restoration efforts. Our results
95 are therefore discussed with respect to the utility of FTIR spectroscopy coupled to
96 predictive PLS in the assessment of organic matter quality with peatland regeneration.

97

98 **2. Materials and Methods**

99 *2.1. Sampling procedure*

100 Sites within gradients of unaided regeneration were selected in previously cut-
101 over peatlands in five countries in Europe (Table 1). Cores ($n = 3$) were obtained from
102 each site with a double-skinned peat corer (to avoid compaction) and were sectioned
103 into 4 horizons of different stages of decomposition. The horizons were designated

104 horizons 3 (surface layer 0-5 cm), 4 (5-10 cm), 6 (22.5-27.5 cm) and 8 (42.5 to 47.5
105 cm). Core samples were cut into 1 cm³ subsamples and the subsamples mixed to
106 ensure homogeneity. Portions were shipped on ice packs to partner laboratories for the
107 relevant analyses contributing to this study. For the purpose of this comparative study,
108 only a single replicate from each Country x Site x Horizon combination was analysed
109 for all analytes. Samples where not all analyses could be completed due to low sample
110 size were excluded from statistical analyses, reducing the dataset for statistical
111 analyses to $n = 68$ (Table 1).

112

113 2.2. FTIR spectroscopy

114 Spectral characterisation of peat samples was performed by diamond
115 attenuated total reflectance FTIR spectroscopy using a Nicolet Magna-IR 550 FTIR
116 spectrometer (Thermo Electron, Warwick, U.K.) fitted with a potassium bromide
117 beam splitter and a deuteroglycine sulphate detector. A Diamond Attenuated Total
118 Reflectance (DATR) accessory, with a single reflectance system, was used to produce
119 transmission-like spectra. The samples were dehydrated by freeze drying and
120 powdered by ball milling with zirconium balls. Samples were placed directly on a
121 DATR/KRS-5 crystal and a flat tip powder press was used to achieve even
122 distribution and contact. Spectra were acquired by averaging 200 scans at 4 cm⁻¹
123 resolution over the range 4000 – 350 cm⁻¹. A correction was made to spectra for the
124 ATR to allow for differences in depth of beam penetration at different wavelengths
125 (Omnic software, version 7.2, Thermo Electron). All spectra were also corrected for
126 attenuation by water vapour and CO₂. Minor differences in the amplitude and baseline
127 between runs were corrected by normalisation of the data by subtraction of the sample
128 minimum followed by division by the average of all data points per sample. First and

129 second derivatives were calculated to determine and test correlations of organic matter
130 variables which formed ‘shoulders’ rather than distinct peaks in the FTIR profiles.

131

132 *2.3. Micromorphological analysis*

133 Micromorphological identification and quantification of peat microremains
134 were carried out using a DMR XP Leica photonic microscope under transmitted light.
135 Wet bulk peat samples were mounted as smear slides and analysed with $\times 20$ and $\times 50$
136 objectives. The surfaces of the main categories were counted (in relative numeric
137 frequencies) through a grid reticule, used as surface unit, and placed on the
138 microscope ocular. Three thousand to 5000 items per sample were counted with an
139 estimated counting error of about 10%.

140

141 *2.4. C and N determination*

142 Carbon and nitrogen contents were determined by combustion at 1100°C with
143 a CNS-2000 LECO apparatus, on dried and crushed peat samples. Due to the total
144 lack of carbonates, total carbon (TC) was assumed to be total organic carbon (TOC).

145

146 *2.5. Characterisation of carbohydrate signatures*

147 Carbohydrate analyses were generally performed on fine-grained peat
148 fractions ($<200\ \mu\text{m}$, isolated by wet-sieving at $200\ \mu\text{m}$ under positive pressure using
149 water circulation), although bulk peat samples were also analysed in some cases, for
150 comparison. Cellulosic and hemicellulosic sugars were identified and quantified by
151 gas chromatography after appropriate hydrolysis. Total sugars were determined by
152 hydrolysis after treatment with concentrated acid (see below) whereas labile
153 (hemicellulosic) sugars were determined independently without this treatment.

154 Cellulosic sugars were determined by difference between the total and
155 hemicellulosic sugars. A detailed procedure is given in Comont et al. (2006). Briefly:
156 for total sugar determination, 1 ml of 24 N H₂SO₄ was added to 100 mg sample dry
157 weight. After 12 h at room temperature, samples were diluted to 1.2 M H₂SO₄ and
158 heated at 100°C for 4 h (hemicellulosic sugar analysis begins directly at this
159 hydrolysis stage). After cooling, deoxy-6-glucose was added as an internal standard
160 and samples were neutralised with CaCO₃. Precipitate was discarded removed
161 following centrifugation and the supernatant evaporated to dryness. After
162 resuspension in methanol, the solution was purified by centrifugation and the
163 supernatant transferred and evaporated under vacuum. The resulting carbohydrates
164 were dissolved in trimethylsilylated pyridine (Sylon BFT, Supelco) and immediately
165 analysed by GC-FID using a 25 m x 0.25 mm CPSil5CB (0.25 µm film thickness)
166 column. Oven settings were as follows: an initial oven temperature (60°C) was
167 ramped at 30°C min⁻¹ to 120°C where it was maintained for 1 min, then ramped to
168 240°C at 3°C min⁻¹ and finally at 20°C min⁻¹ up to 310°C where it was maintained for
169 10 min. The injector split was off at the start time and turned on after 2 min. The
170 injector and detector were maintained at 240°C and 300°C, respectively. A mixture of
171 eight monosaccharides (ribose, arabinose, xylose, rhamnose, fucose, glucose,
172 mannose and galactose) was used as an external standard for compound identification
173 through peak retention times and for individual response coefficient determination.
174

175 2.6. Statistical analyses

176 All statistical analyses were performed using Genstat for Windows (8th
177 edition, VSN International). FTIR spectral data in the diamond interference region
178 (2200-1900 cm⁻¹) were excluded from analyses. Relationships between FTIR spectra
179 ('x' variate, as zero, first and second order derivatives) and the corresponding organic

180 matter (micromorphological and carbohydrate signature) datasets as well as carbon
181 and nitrogen contents and their ratios ('y' variates) were assessed using partial least
182 squares (PLS) analyses. We investigated both each parameter separately in univariate
183 PLS and also within multivariate datasets in multivariate PLS, with leave-one-out
184 validation. The Genstat procedure returned the number of latent roots (dimensions),
185 the predicted residual error sum of squares (PRESS), percentage of variance explained
186 and PLS loadings. The number of roots for each PLS analysis was set at the number
187 that returned minimum PRESS. The root mean square error of cross-validation
188 (RMSECV) was calculated from PRESS using the square root of $PRESS/n$.
189 Significance levels were estimated using Osten's F-test. Assessment of the predictive
190 qualities of PLS was performed by principal component analysis (PCA) of the
191 observed and predicted values for both micromorphological analyses and plant-
192 derived carbohydrate monomer signatures.

193

194 **3. Results**

195 *3.1. Patterns of FTIR carbon chemistry signatures*

196 Sample characterisation using FTIR spectroscopy concerned the correct
197 assignment of the observed spectral characteristics to the most likely origin of the
198 absorption bands. A summary of the most characteristic bands observed in peat and
199 their assignment is presented in Table 2. Generally, FTIR analysis on the peat horizon
200 samples showed a decline of the main polysaccharide markers (absorption bands
201 around 3400 and 1040 cm^{-1}) and relative increase of the main bands assigned to
202 lignin-like (1513, 1450, 1371, 1265 and 835 cm^{-1}) and aliphatic structures (2920 and
203 2850 cm^{-1}) with depth, as expected with increasing humification. Figure 1 shows an
204 example from a Scottish peat core at an advanced stage of regeneration. Spectral
205 bands indicative of 'carboxylates', which include contributions from vibrations of

206 aromatic and aliphatic carboxylates ($R\text{-COO}^-$) and/or aromatic $C=C$ structures also
207 increased in relative terms with depth (1650-1600 and 1426 cm^{-1}).

208

209 *3.2. PLS calibrations with chemical and organic matter parameters*

210 The FTIR data were assessed against the data obtained from organic matter
211 analyses (variation of the original data shown in Table 3) using both univariate and
212 multivariate PLS analyses. In the cases of the elemental and carbohydrate analyses,
213 the percentage variance explained was $> 60\%$ for the majority of the analytes (Table
214 4) and all were highly significant in PLS of the zero order FTIR data. PLS using the
215 first or second derivative did increase the percentage variance explained, but only
216 marginally (data not shown). The RMSECV values (Table 4) were generally lower
217 than the standard deviation of the original datasets (Table 3). Total C content was
218 associated with positive loadings in the main polysaccharide envelopes at 3300 and
219 1030 cm^{-1} and negative loadings of the wax markers at 2920 and 2850 cm^{-1} (Fig. 2A).
220 Total N content was associated with positive loadings in the bands representing the
221 amide I and II regions (Table 2) as previously reported by Chapman et al (2001) and
222 there an additional negative correlation with the wax markers at 2920 and 2850 cm^{-1}
223 (Fig 2B). The loading plots for hemicellulosic sugars (Fig 2C) showed a similar
224 positive relationship with the main polysaccharide bands but there was also a strong
225 negative relationship with the carboxylate marker region. Loadings generated for
226 fucose (Fig 2D) primarily demonstrated a strong negative correlation with the wax
227 markers at 2920 and 2850 cm^{-1} .

228 In some cases, the differences in loadings were more subtle. For example, the
229 PLS loadings for mucilage were visually very similar to those of total C content (not
230 shown). We therefore also examined the relative differences in PLS loadings between
231 organic matter parameters using subtraction. Examples of relative differences in PLS

232 loadings are shown in Fig 3. The relative difference in PLS loadings between those
233 generated for mucilage and those for total C (Fig 3A) showed that both the main
234 polysaccharide envelope around 1100 cm^{-1} and the wax markers (2920 and 2850 cm^{-1})
235 were less discriminatory for prediction of mucilage content than for total C. Similarly,
236 for the prediction of structureless *Cyperaceae* versus preserved *Cyperaceae*, the wax
237 marker bands and various other bands indicative of more humified tissue (1710 - 1707 ,
238 1650 - 1600 , and 1515 - 1513 cm^{-1}) were more discriminatory (Fig 3B). For most neutral
239 sugars, however, the main discriminatory region was within the main 1200 - 800 cm^{-1}
240 polysaccharide envelope (Fig 3C-F). Within this polysaccharide envelope, there were
241 subtle differences in the bands which contributed more or less to the discrimination
242 between different neutral sugars.

243

244 *3.3. Predictive PLS of FTIR spectra as a tool in organic matter studies of* 245 *regenerating peatlands*

246 To assess the potential of predictive PLS of FTIR spectra for organic matter
247 parameters, we reconstructed the composition of the organic matter datasets (i.e.
248 micromorphological fingerprints, carbohydrate signatures) using the PLS outputs.
249 Examples of the changes of the organic matter parameters and correlation with the
250 predicted values with depth are shown for two contrasting sites of the peatland at Le
251 Russey, France (Fig. 4). The fitted and observed values were in close agreement for
252 the carbohydrate parameters.

253 Over the entire dataset of 68 samples from all sites in Europe, values for the
254 observed versus predicted C:N ratio's were highly correlated and linear regression
255 explained 70.6 % of the variance (Fig 5A). To test whether PLS analyses were
256 adequate in predicting the organic matter composition of each of the peat samples, we
257 combined the predicted values from univariate PLS analyses for each subset of

258 multivariate organic matter analyses (i.e. micromorphological and carbohydrates) and
259 analysed these reconstructed organic matter datasets using PCA. We subsequently
260 compared them to PCA of the observed OM characteristics using linear regression of
261 the 1st principal components (Fig. 5B and C). Linear regression explained 51.0 and
262 82.1 % of the variance in comparisons of the first principal components of the
263 micromorphological and carbohydrate composition obtained by univariate PLS
264 models, respectively (Fig. 5B and C). We also tested the predicted values of
265 multivariate PLS. The regressions of multivariate PLS explained a marginally lower
266 percentage of the variance in the datasets (data not shown). The first principal
267 components of the carbohydrate datasets explained the majority of the variance in
268 both the observed and fitted datasets (88.7 and 94.9 %, respectively). The observed
269 strength of the regression therefore indicates that PLS is able to predict the
270 carbohydrate signature of a wide range of peat samples.

271

272 **4. Discussion**

273 *4.1. FTIR spectral characteristics and the potential effect of spectral interferences on* 274 *PLS models*

275 We observed a few samples which showed spectral interference from silicate
276 minerals. A notable example is shown in Fig 1A in the Scottish sample from an
277 advanced stage of regeneration at horizon 6 (22.5-27.5 cm depth), which shows the
278 diagnostic peaks at 3700 and 467 cm⁻¹ of kaolinite. Where mineral interferences
279 manifest themselves in samples obtained from deeper horizons, they may have
280 originated from wind-blown material from nearby exposed mineral surfaces during
281 the formation of the peatlands. We also observed spectral signals from silicate
282 minerals in a few surface samples from sites on, or close to, nearly exhausted
283 peatlands. Mineral interference also manifests itself in the 1030 cm⁻¹ polysaccharide

284 band (Farmer, 1974) and could therefore potentially skew the accuracy of prediction
285 of the polysaccharide markers. Other notable results were the low relative absorption
286 values in the 1707 cm^{-1} region in the samples from the Baupte peatland (data not
287 shown). Peat samples from Baupte had consistently higher pH values and we
288 therefore attributed this lack of absorption in the 1707 cm^{-1} region to the majority of
289 acids being present in the carboxylate form. A reduction in intensity of the 1720 cm^{-1}
290 absorption band with increasing pH values was been previously shown in FTIR
291 analyses on peat samples where the sample pH was moderated (Gondar et al., 2005).
292 In low pH environments however, for example as observed in the profile of the
293 Scottish peat samples (e.g. Fig.1), this variation is related to peat decomposition rather
294 than pH changes and increases in intensity of this band illustrate progressive free acid
295 release with increasing humification. Analysis without samples that were
296 characterised by spectral interference by silicate minerals, or those with elevated pH
297 values, did not increase the amount of variability explained by PLS (data not shown).

298

299 *4.2. Principal calibrations*

300 Infrared spectroscopic data from peat samples, both in the mid and near IR
301 ranges, have been used previously to predict various organic matter parameters. Good
302 correlations by PLS between various parameters such as total C and N, pH, ash
303 content, total organic matter etc, and IR analyses of organic soils have been shown on
304 numerous occasions (Palmborg and Nordgren, 1993; Chapman et al., 2001; Tremblay
305 and Gagne, 2002, Couteaux et al., 2003). Some studies have attempted to predict a
306 small range of functional chemical signatures of peat, such as relative concentrations
307 of amino acids and amino sugars (Holmgren and Norden, 1988) or humic and fulvic
308 acids (Tremblay and Gagne, 2002). The use of ATR accessories produces more
309 consistent data and the use of an additional water correction has been shown to

310 increase the accuracy of total C predictions (Tucker et al., 2001). A possible reason
311 for the generally poor relationships of FTIR data with micromorphological analyses
312 may be the size of sample used in direct microscopic analysis compared to the use of
313 a homogenised sample as for FTIR spectroscopy. Another possible factor is the three-
314 dimensionality of the chemical analyses (as these are based on mass), compared to
315 micromorphological analyses which essentially extrapolate the mass of microremains
316 based on the area they occupy within smearslices. The variance explained by PLS
317 with some of the more prevalent tissues observed (e.g. proportion of preserved
318 *Cyperaceae* and mucilage) are generally more encouraging (Table 4). Other reports
319 have, however, shown the ability to separate major vegetational differences using near
320 infrared spectroscopy, where the authors were able to build good PLS models with
321 high levels of explained variance for the content of leaf material from Ericales and
322 *Sphagnum* spp. in a single peat core sectioned to 1 cm samples (McTiernan et al.,
323 1998). In the near infra-red, the vibrational characteristics of the N-H and O-H stretch
324 regions are more separated, while the mid-IR is dominated by the O-H stretch regions.
325 Use of data from near infrared analyses may therefore improve the prediction of
326 organic matter parameters.

327 We also observed cases where the variance explained within the carbohydrate
328 parameters was rather low (Table 4). The carbohydrate chemistry was assessed on the
329 fine fraction (< 200 micron) because this size fraction offers greater sensitivity as it is
330 composed of the biodegraded plant material admixed with products of secondary
331 microbial production. The bulk fraction signature is effectively ‘swamped’ by intact
332 or only partially degraded plant tissues (Comont et al., 2006). This may, however,
333 also offer an explanation for the relatively low variance explained for the total
334 cellulosic sugar content as well as the relative amounts of arabinose and xylose by
335 PLS on the bulk sample derived FTIR data. The latter monomers are the principal

336 biomarkers of sedges (e.g. *Cyperaceae*; Moers et al., 1989; Comont et al., 2006),
337 which in most samples appear to be the dominant preserved tissues (Table 3).
338 Similarly, single correlations for each of the principal biomarkers of intact
339 bryophytes, mannose, rhamnose and galactose (Popper and Fry, 2003) were rather
340 poor (Table 3). FTIR spectroscopy has been successfully used previously to predict
341 the neutral sugar monomers of plant cell wall polysaccharides in foodstuffs, including
342 such monomers as those described as vegetation biomarkers in peatlands. Examples
343 are prediction of mannose content (from mannans and mannoproteins) in wines
344 (Coimbra et al., 2005) and xylose content from olive pulp polysaccharides (Coimbra
345 et al., 1999). That we were able to successfully reassemble the neutral sugar profiles
346 (Fig. 5) of a large variety of peatland samples from five European locations with large
347 differences in plant cover and degree of decomposition despite observing low
348 correlation of each principal monomer with FTIR spectra may at first seem puzzling.
349 Kačuráková et al. (2000) investigated individual plant cell wall compounds (pectic
350 polysaccharides, hemicelluloses and monosaccharides) by FTIR spectroscopy and were
351 able to determine spectral marker regions for a large number of these compounds
352 within the 1200-800 cm^{-1} region. They attributed the main differences to both C-OH
353 relative steric positions within the monomer side chains as well as the vibrational
354 characteristics of the pyranose backbones. Carbohydrate analysis reports on the
355 individual components of each (hemi)cellulose type present in the more biologically
356 decomposed size fractions, whereas the FTIR spectra report on the spectral properties
357 of both the side-chain monomers and the pyranose backbones. In agreement with
358 Kačuráková et al., we showed in this study that the spectral markers within the 1200-
359 800 cm^{-1} region were discriminatory for the relative differences in PLS prediction
360 between neutral sugars (Fig. 3). The correlation of the multivariate datasets is

361 therefore most likely explained by both methodologies essentially reporting on the
362 original composition of the parent vegetational material.

363

364 *4.3. Predictive potential of peat FTIR-based PLS models and applications in*
365 *restoration monitoring*

366 The main strength of this study is the ability to satisfactorily reconstruct (Fig.
367 5) the relative differences between peat samples from different stages of regeneration
368 and from widely differing locations with their associated differences in vegetation
369 structures, and hence micromorphological and chemical composition. In peatland
370 restoration projects, it is often difficult to ascertain the regeneration boundary, i.e. the
371 interphase between the cut horizon of remaining catotelm and the accumulated
372 organic matter during regeneration. The C:N ratio and micromorphological
373 composition of peat have been previously used as an indicator of this regeneration
374 boundary by Comont et al., (2006). The composition of carbohydrate monomers is
375 also indicative of the origin of the OM (i.e. vegetation-type specific, Moers et al.,
376 1989; Wicks et al., 1991) and fucose has been proposed as an indicator of microbially
377 produced polysaccharide monomers (Murayama et al., 1988; Comont et al., 2006). A
378 simple ratio of the polysaccharide to carboxylate FTIR band intensity has previously
379 been shown to explain 68.7 % of the community catabolic response to a suite of
380 simple carbon sources (Artz et al., 2006) and other studies have shown good
381 predictive properties of PLS analyses on FTIR and NIR data with microbial biomass
382 (Chapman et al., 1998; Couteaux et al., 2003). There are other reports where IR data
383 have been used in prediction of various organic matter parameters such as cellulose
384 content and cellulose decomposition rates (Hartmann and Appel, 2006) or the relative
385 quantities of phenolic compounds and leaf litter decomposition rates (Stolter et al.,
386 2006). The botanical composition of peat, i.e. the composition of litter entering the

387 organic matter pool, has been implicated in the degree of decomposition on numerous
388 occasions (Verhoeven and Toth, 1995; Belyea, 1996; Froelking et al., 2001) and
389 therefore the composition of the organic matter in restored peatlands may be critical to
390 their long term carbon sequestration potential. Indeed, Andersen et al. (2006) showed
391 that the substrate quality (in terms of availability of N, P and soluble organic carbon)
392 of the organic matter in vegetational successions on cutover peatlands was related to
393 the evolution of the total microbial biomass and their respiration activity. Therefore,
394 monitoring of restoration projects should include evaluations whether organic matter
395 parameters return to values more closely resembling intact peatland systems. FTIR
396 spectroscopy coupled with predictive PLS analysis may be a useful, low-cost,
397 addition to the toolbox in the assessment and monitoring of restoration success in
398 peatland ecosystems.

399

400

Acknowledgements

This work was part of the RECIPE initiative, funded through a grant by the EU Framework 5. SJC is funded by the Scottish Executive Environment and Rural Affairs Department. The authors gratefully acknowledge analytical assistance provided by M. Hatton and N. Lottier. We would like to thank Dr. David Elston (BioSS) and Dr. Charlie Shand (Macaulay Institute) for constructive comments on this manuscript.

References

- Andersen, R., Francez, A.-J., Rochefort, L., 2006. The physicochemical and microbiological status of a restored bog in Québec: Identification of relevant criteria to monitor success. *Soil Biology and Biochemistry* 38, 1375-1387.
- Artz, R.R.E., Chapman, S.J., Campbell, C.D. 2006. Substrate utilisation profiles of microbial communities in peat are depth dependent and correlate with whole soil FTIR profiles. *Soil Biology and Biochemistry* 38, 2958-2962.
- Bjarnestad, S., Dahlman, O. 2002. Chemical compositions of hardwood and softwood pulps employing photoacoustic Fourier transform infrared spectroscopy in combination with partial least-squares analysis. *Analytical Chemistry* 74, 5851-5858.
- Belyea, L.R. 1996. Separating the effects of litter quality and microenvironment on decomposition rates in a patterned peatland. *Oikos* 77, 529-539.
- Bourdon, S., Laggoun-Défarge F., Disnar, J.-R., Maman, O., Guillet, B., Derenne, S., Largeau, C., 2000. Organic matter sources and early diagenetic degradation in a tropical peaty marsh (Tritrivakely, Madagascar). Implications for environmental reconstruction during the Sub-Atlantic. *Organic Geochemistry* 31, 421-438.
- Chapman, S.J., Buttler, A., Francez, A.-J., Laggoun-Defarge, F., Vasander, H., Schloter, M., Combe, J., Grosvernier, P., Harms, H., Epron, D., Gilbert, D., Mitchell, E.A.D. 2003. Exploitation of northern peatlands and biodiversity maintenance: a conflict between economy and ecology. *Frontiers in Ecology and Environment* 1, 525-532.

- Chapman, S.J., Campbell, C.D., Fraser, A.R., Puri, G., 2001. FTIR spectroscopy of peat in and bordering Scots pine woodland: relationships with chemical and biological properties. *Soil Biology and Biochemistry* 33, 1193-1200.
- Cheshire, M.V. 1979. *Nature and origin of carbohydrates in soil*. Academic Press, London.
- Cocozza, C., D'Orazio, V., Miano, T.M., Shotyk, W. 2003. Characterization of solid and aqueous phases of a peat bog profile using molecular fluorescence spectroscopy, ESR and FT-IR, and comparison with physical properties. *Organic Geochemistry* 34, 49-60.
- Coimbra, M.A., Barros, A.S., Coelho, E., Goncalves, F., Rocha, S.M., Delgadillo, I. 2005. Quantification of polymeric mannose in wine extracts by FT-IR spectroscopy and OSC-PLS1 regression. *Carbohydrate Polymers* 61, 434-440.
- Coimbra, M.A., Barros, A.S., Rutledge, D.N., Delgadillo, I. 1999. FTIR spectroscopy as a tool for the analysis of olive pulp cell-wall polysaccharide. *Carbohydrate Research* 317, 145-154.
- Comont, L., Laggoun-Défarge, F., Disnar, J.-R. 2006. Evolution of organic matter indicators in response to major environmental changes : the case of a formerly cutover peatbog (Le Russey, Jura Mountains, France). *Organic Geochemistry* (In press).
- Couteaux, M.M., Berg, B., Rovira, P. 2003. Near infrared reflectance spectroscopy for determination of organic matter fractions including microbial biomass in coniferous forest soils. *Soil Biology and Biochemistry* 35, 1587-1600.

- Durig, D.T., Esterle, J.S., Dickson, T.J., Durig, J.R. 1988. An Investigation of the Chemical Variability of Woody Peat by FT-IR Spectroscopy. *Applied Spectroscopy* 42, 1239-1244
- Farmer, V.C. The Infrared spectra of minerals. Mineralogical Society Monograph 4. Mineralogical Society London, 1974.
- Freeman, C., Evans, C.D., Monteith, D.T., Reynolds, B., Fenner, N., 2001. Export of organic carbon from peat soils. *Nature* 412, 785.
- Frolking, S.E., Bubier, J.L., Moore, T.R., Ball, T., Bellisario, L.M., Bhardwaj, A., Carroll, P., Crill, P. M., Lafleur, P. M., McCaughey, J. H., Roulet, N. T., Suyker, A., Verma, S. B., Waddington, J. M., Whiting, G. J. 1998. Relationship between ecosystem productivity and photosynthetically active radiation for northern peatlands. *Global Biogeochemical Cycles* 12, 115-126.
- Glatzel, S., Kalbitz, K., Dalva, M., Moore, T., 2003. Dissolved organic matter properties and their relationship to carbon dioxide efflux from restored peat bogs. *Geoderma* 113, 397-411.
- Gondar, D., Lopez, R., Fiol, S., Antelo, J.M., Arce, F. 2005. Characterization and acid-base properties of fulvic and humic acids isolated from two horizons of an ombrotrophic peat bog. *Geoderma* 126, 367-374.
- Gonzalez, J.A., Gonzalez-Vila, F.J., Almendros, G., Zancada, M.C., Polvillo, O., Martin, F. 2003. Preferential accumulation of selectively preserved biomacromolecules in the humus fractions from a peat deposit as seen by analytical pyrolysis and spectroscopic techniques. *Journal of Analytical and Applied Pyrolysis* 68, 287-298.

- Gorham, E., 1991. Northern peatlands: Role in the carbon cycle and probable responses to climatic warming. *Applied Soil Ecology* 1, 182-195.
- Gorham, E., Rochefort, L. 2003. Peatland restoration: A brief assessment with special reference to Sphagnum bogs. *Wetlands Ecology and Management* 11, 109-119.
- Guo, Y., Bustin, R.M. 1998. FTIR spectroscopy and reflectance of modern charcoals and fungal decayed woods: implications for studies of inertinite in coals. *International Journal of Coal Geology* 37, 29-53.
- Haberhauer, G., Feigl, B., Gerzabek, M.H., Cerri, C. 2000. FT-IR spectroscopy of organic matter in tropical soils: Changes induced through deforestation. *Applied Spectroscopy* 54, 221-224.
- Haberhauer, G., Gerzabek, M.H., 1999. Drift and transmission FT-IR spectroscopy of forest soils: an approach to determine decomposition processes of forest litter. *Vibrational Spectroscopy* 19, 413-417.
- Haberhauer, G., Rafferty, B., Strebl, F., Gerzabek, M.H., 1998. Comparison of the composition of forest soil litter derived from three different sites at various decompositional stages using FTIR spectroscopy. *Geoderma* 83, 331-342.
- Hartmann, H.P., Appel, T. 2006. Calibration of near infrared spectra for measuring decomposing cellulose and green manure in soils. *Soil Biology and Biochemistry* 38, 887-897.
- Holmgren, A., Norden, B. 1988. Characterization of peat samples by diffuse reflectance FT-IR spectroscopy. *Applied Spectroscopy* 42, 255-262.
- Ibarra, J.V., Munoz, E., Moliner, R. 1996. FTIR study of the evolution of coal structure during the coalification process. *Organic Geochemistry* 24, 725-735.

- Kačuráková, M., Capek, P., Sasinkova, V., Wellner, N., Ebringerova, A. 2000. FT-IR study of plant cell wall model compounds: pectic polysaccharides and hemicelluloses. *Carbohydrate Polymers* 43, 195-203.
- McTiernan, K.B., Garnett, M.H., Mauquoy, D., Ineson, P., Couteaux, M.M. 1998. Use of near-infrared reflectance spectroscopy (NIRS) in palaeoecological studies of peat. *Holocene* 8, 729-740.
- Moers, M.E.C., Baas, M., de Leeuw, J.W., Boon, J.J., Schenck, P.A., 1990. Occurrence and origin of carbohydrates in peat samples from a red mangrove environment as reflected by abundances of neutral monosaccharides. *Geochimica et Cosmochimica Acta* 54, 2463-2472.
- Moers, M.E.C., Boon, J.J., de Leeuw, J.W., Baas, M., Schenck, P.A. 1989. Carbohydrate speciation and Py-MS mapping of peat samples from a subtropical open marsh environment. *Geochimica et Cosmochimica Acta* 53, 2011-2021.
- Murayama, S., 1988. Microbial synthesis of saccharides in soils incubated with ¹³C-labelled glucose. *Soil Biology and Biochemistry* 20, 193-199.
- Niemeyer, J., Chen, Y., Bollag, J.M. 1992. Characterization of humic acids, composts, and peat by diffuse reflectance Fourier-Transform infrared-spectroscopy. *Soil Science Society of America Journal* 56, 135-140.
- Palmborg, C., Nordgren, A. 1993. Modelling microbial activity and biomass in forest soil with substrate quality measured using near infrared reflectance spectroscopy. *Soil Biology and Biochemistry* 25, 1713-1718.
- Parker, F.S. Applications of infrared spectroscopy in biochemistry, biology and medicine. Adam Hilger, London, 1971.

- Popper Z.A., Fry S.C., 2003. Primary cell wall composition of bryophytes and charophytes. *Annals of Botany* 91, 1-12.
- Stolter, C., Julkunen-Tiitto, R., Ganzhorn, J. 2006. Application of near infrared reflectance spectroscopy (NIRS) to assess some properties of a sub-arctic ecosystem. *Basic and Applied Ecology* 7, 167-187.
- Tremblay, L., Gagne, J.-P. 2002. Fast quantification of humic substances and organic matter by direct analysis of sediments using DRIFT spectroscopy. *Analytical Chemistry* 74, 2985-2993.
- Trouvé, C., Disnar, J.-R., Mariotti, A., Guillet, B., 1996. Changes in the amount and distribution of neutral monosaccharides of savanna soils after plantation of *Pinus* and *Eucalyptus* in the Congo. *European Journal of Soil Science* 47, 51-59.
- Tucker, M.P., Nguyen, Q.A., Eddy, F.P., Kadam, K.L., Gedvilas, L.M., Webb, J.D. 2001. Fourier transform infrared quantitative analysis of sugars and lignin in pretreated softwood solid residues. *Applied Biochemistry and Biotechnology* 91, 51-61.
- Tuittila, E.-S., Komulainen, V.-M., Vasander, H., Laine, J., 1999. Restored cut-away peatland as a sink for atmospheric CO₂. *Oecologia* 120, 563-574.
- Verhoeven, J.T.A., Toth, E. 1995. Decomposition of *Carex* and *Sphagnum* litter in fens: Effects of litter quality and inhibition by living tissue homogenates. *Soil Biology and Biochemistry* 27, 271-275.
- Waddington, J.M., Warner, K.D. 2001. Atmospheric CO₂ sequestration in restored mined peatlands. *Ecoscience* 8, 359-369.

Wicks, R.J., Moran, M.A., Pittman, L.J., Hodson, R.E. 1991. Carbohydrate signatures of aquatic macrophytes and their dissolved degradation products as determined by a sensitive high-performance ion chromatography method. *Applied and Environmental Microbiology* 57, 3135-3143.

Zaccheo, P., Cabassi, G., Ricca, G., Crippa, L. 2002. Decomposition of organic residues in soil: experimental technique and spectroscopic approach. *Organic Geochemistry* 33, 327-345.

Figure legends:

Fig. 1. FTIR spectra of peat profile samples from the Scottish Site D (an advanced stage of regeneration), ranging from the surface moss layer at 0-5 cm (solid line) through decomposing plant litter at 5-10 cm (dashed line) and highly humified peat at 22.5 - 27.5 cm (dash-dotted line) and at 42.5 - 47.5 cm (dotted line). Relative abundances for each spectral signal were obtained by normalisation of data (see text). Characteristic FTIR bands of the major biochemical descriptors have been marked on the whole spectrum (**A**) and in the region containing the lignin, carboxylate and peptide markers (**B**). The left and right insets represent magnified sections of the spectrum of the 22.5 - 27.5 cm horizon. Spectral markers indicative of mineral interference in this sample have been marked with arrows (see text).

Fig. 2. Loadings generated by partial least squares analysis of zero-order FTIR-ATR absorbances against **A**) Total C and **B**) total N content. Loadings against micromorphological parameters such as percentage preserved (solid line) and structureless (dotted line) *Cyperaceae* tissues and mucilage are shown in Figs. **C** and **D**, respectively. Figures E and F present loadings generated against hemicellulosic sugars and fucose, respectively.

Fig. 3. Relative differences in PLS loadings between different organic matter parameters as assessed by subtraction of loadings. Variations over the entire FTIR spectral range are shown for the differences in loadings between mucilage and total C content (**A**) and the difference between structureless versus preserved *Cyperaceae* (**B**). Relative differences in PLS loadings within the polysaccharide envelope are

characteristic for neutral sugars. Differences in loadings of fucose versus xylose (C), arabinose versus mannose (D), fucose versus ribose (E) and mannose versus rhamnose (F) are shown as examples.

Fig. 4. Fitted (open symbols) versus observed (closed symbols) values for various organic matter parameters with depth (cm) for the site in the early stage of regeneration (FR-A) and the intact site (FR-D) in the peatland at Le Russey, France.

Fig. 5. Predictive properties of univariate PLS models based on FTIR data to describe the following organic matter properties of peat. **A:** Predicted (x) vs. observed (y) values of C/N ratios **B:** Regression plot of the first dimensions of PCA performed on the PLS predicted (x) versus observed (y) values of the micromorphological remains. Each micromorphological parameter was used in separate univariate PLS analyses and the predicted data were used for PCA based reconstruction. Variance explained for the first dimensions for each PCA are shown in brackets on each axis. **C:** Regression plot of the first dimensions of PCA performed on the PLS predicted (x) versus observed (y) values of the carbohydrate monomer analyses. Each carbohydrate parameter was used in separate univariate PLS analyses and the predicted data were used for PCA based reconstruction. Variance explained for the first dimensions for each PCA are shown in brackets on each axis. Samples from the different countries are indicated by the following symbols: Finnish samples (downward, filled triangles), France Baupte (empty circles), France Russey (upward, empty triangles), Switzerland Chaux d'Abel (filled circles) and Scotland (filled squares). The solid lines indicate the mean regression, the dashed lines indicate the 95% confidence interval and the dotted lines indicate the 95% prediction intervals.

Figure 1

[Click here to download high resolution image](#)

Soil Biology and Biochemistry

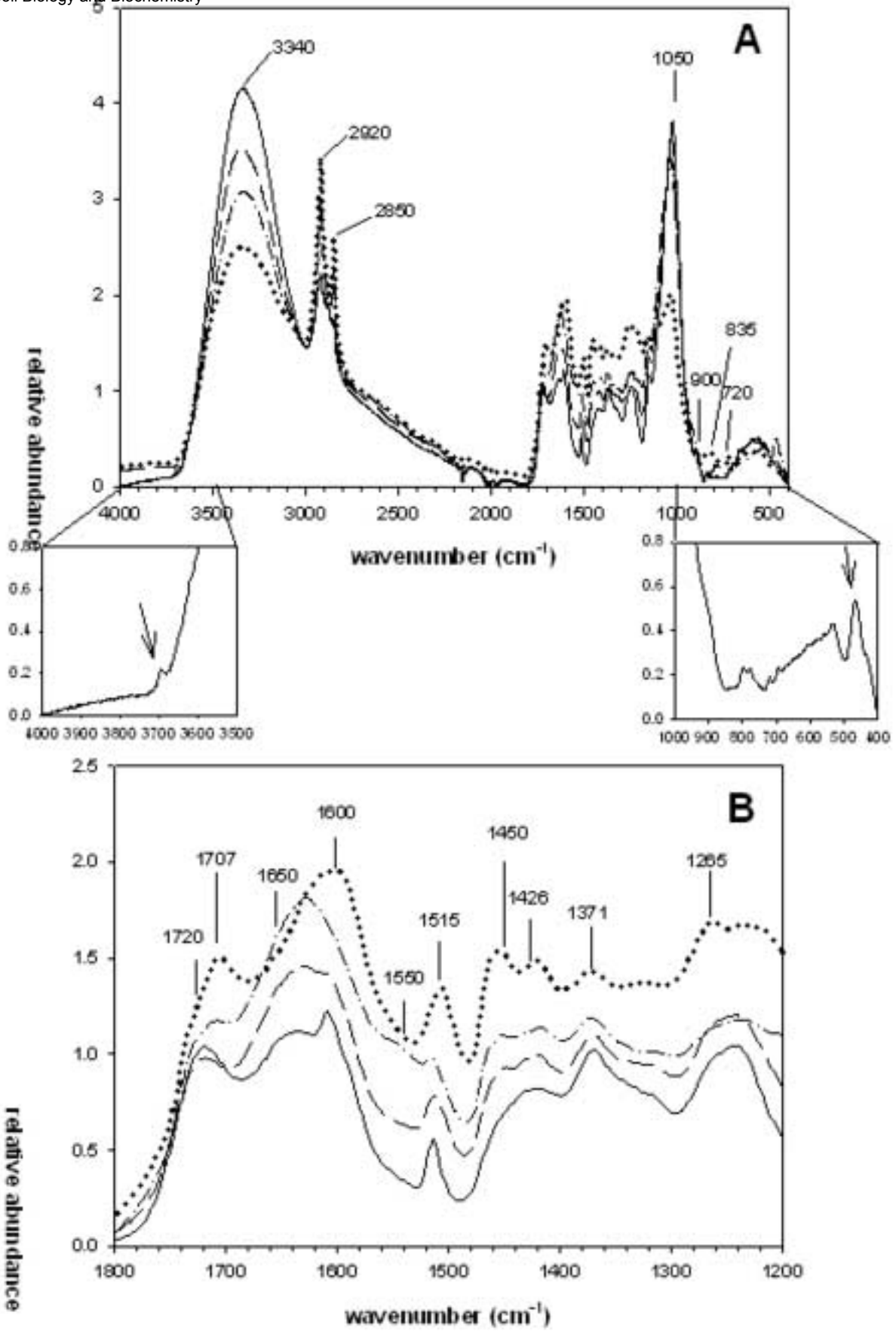


Figure 2

[Click here to download high resolution image](#)

Soil Biology and Biochemistry

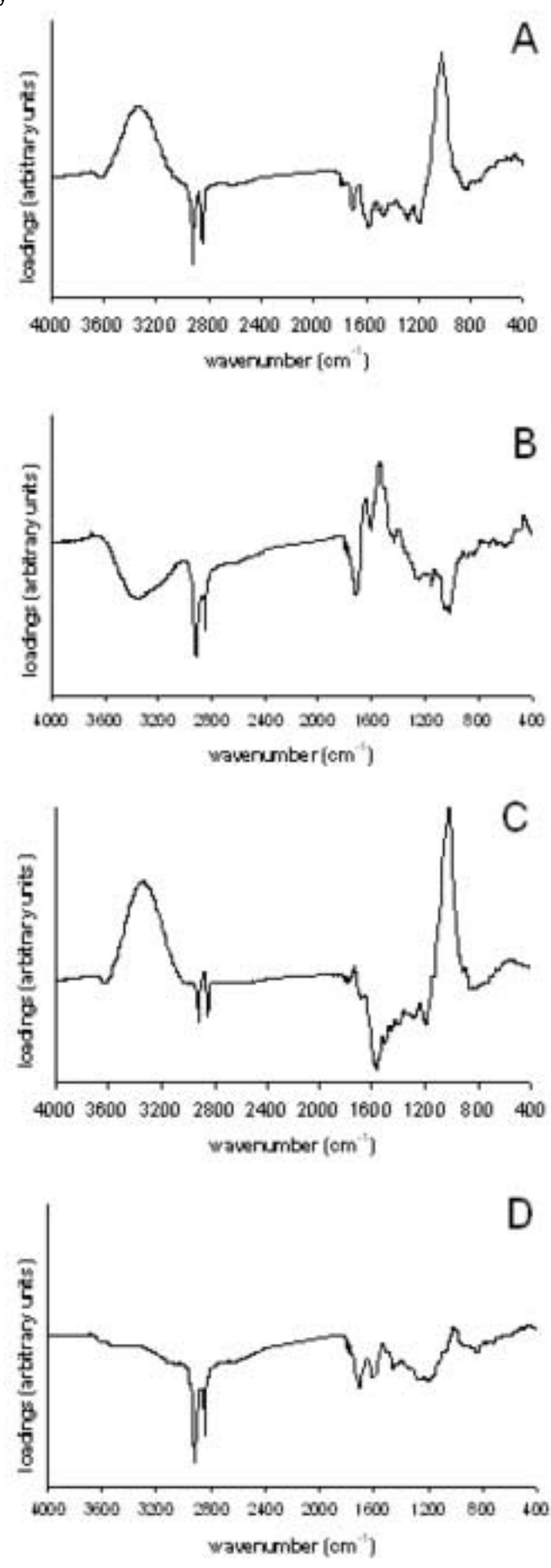


Figure 3

[Click here to download high resolution image](#)

Soil Biology and Biochemistry

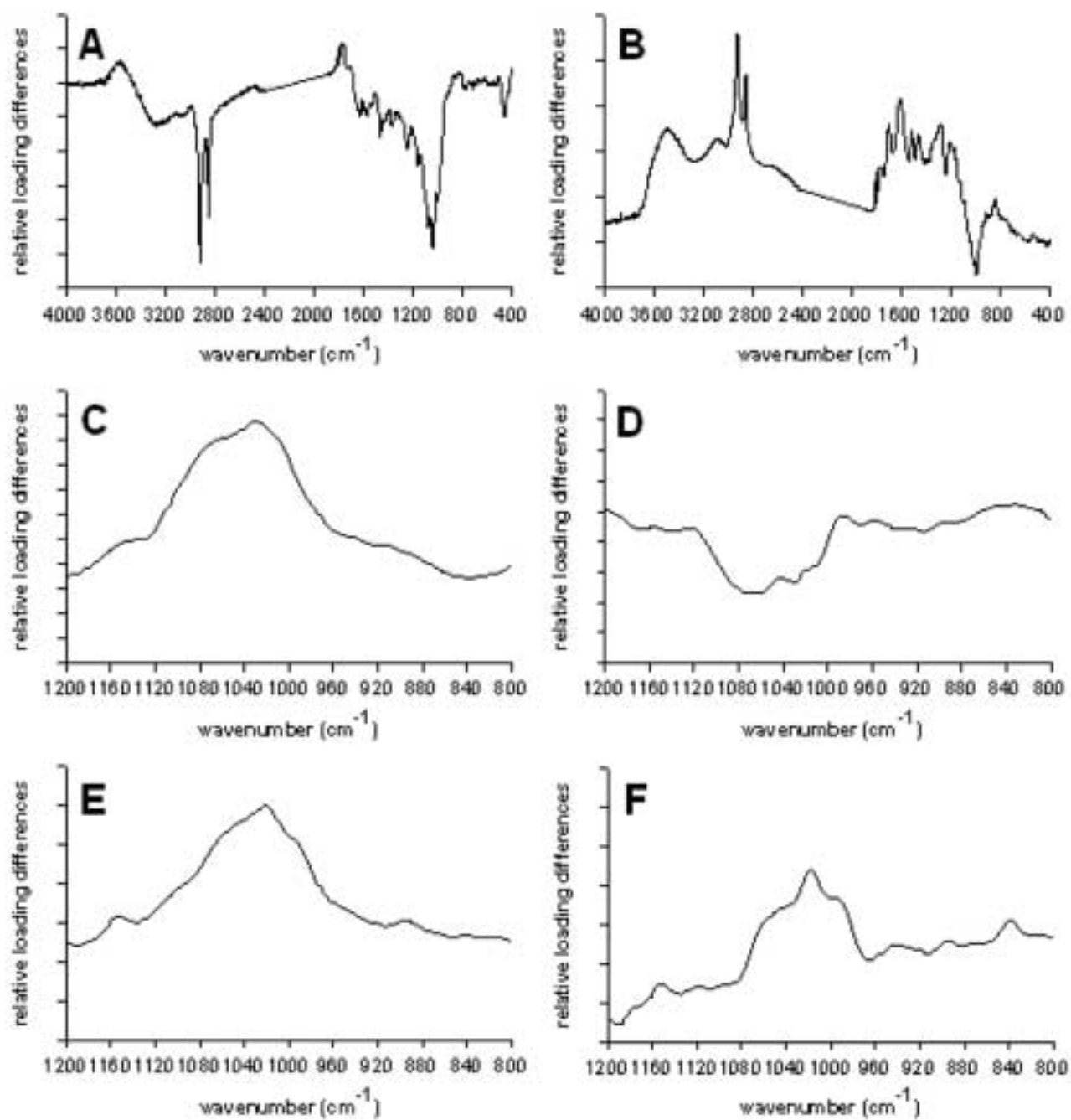


Figure 4

[Click here to download high resolution image](#)

Soil Biology and Biochemistry

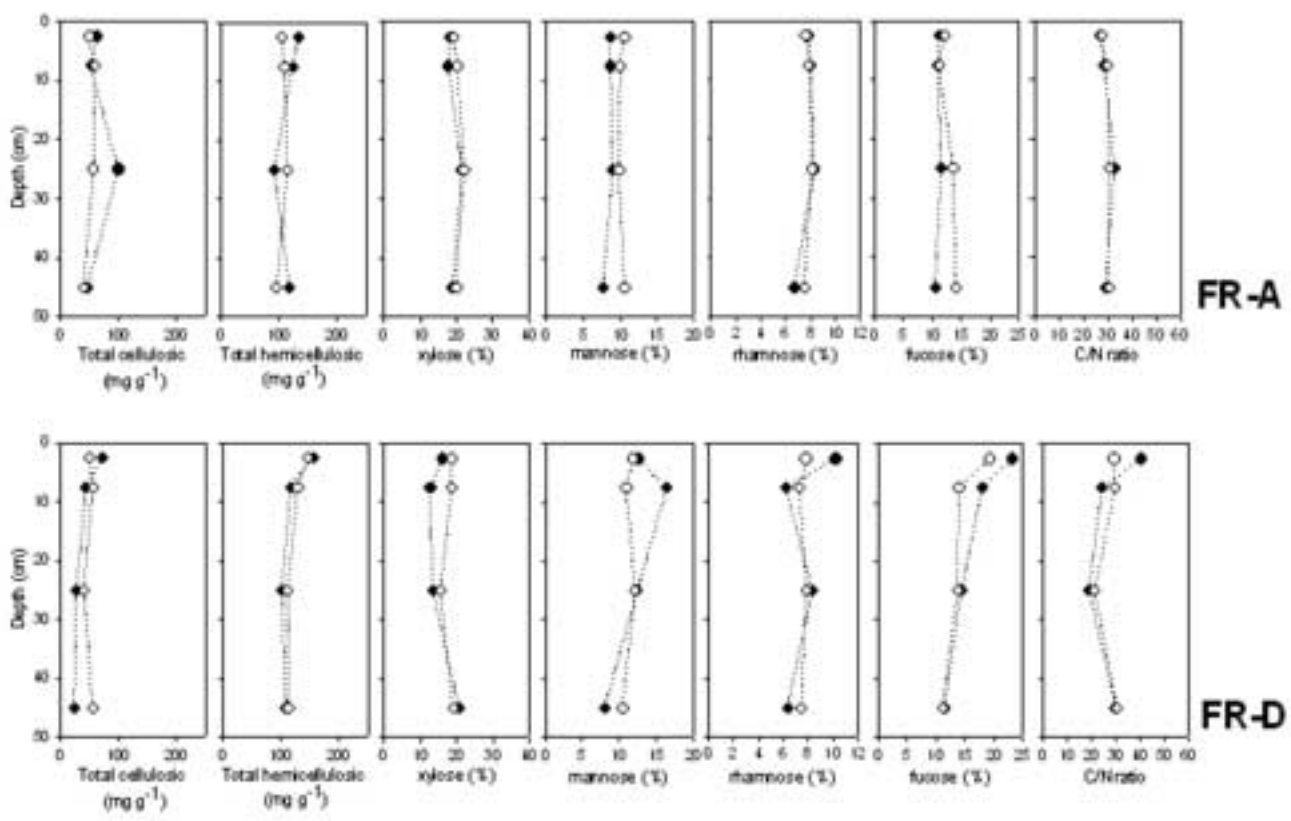


Figure 5

[Click here to download high resolution image](#)

Soil Biology and Biochemistry

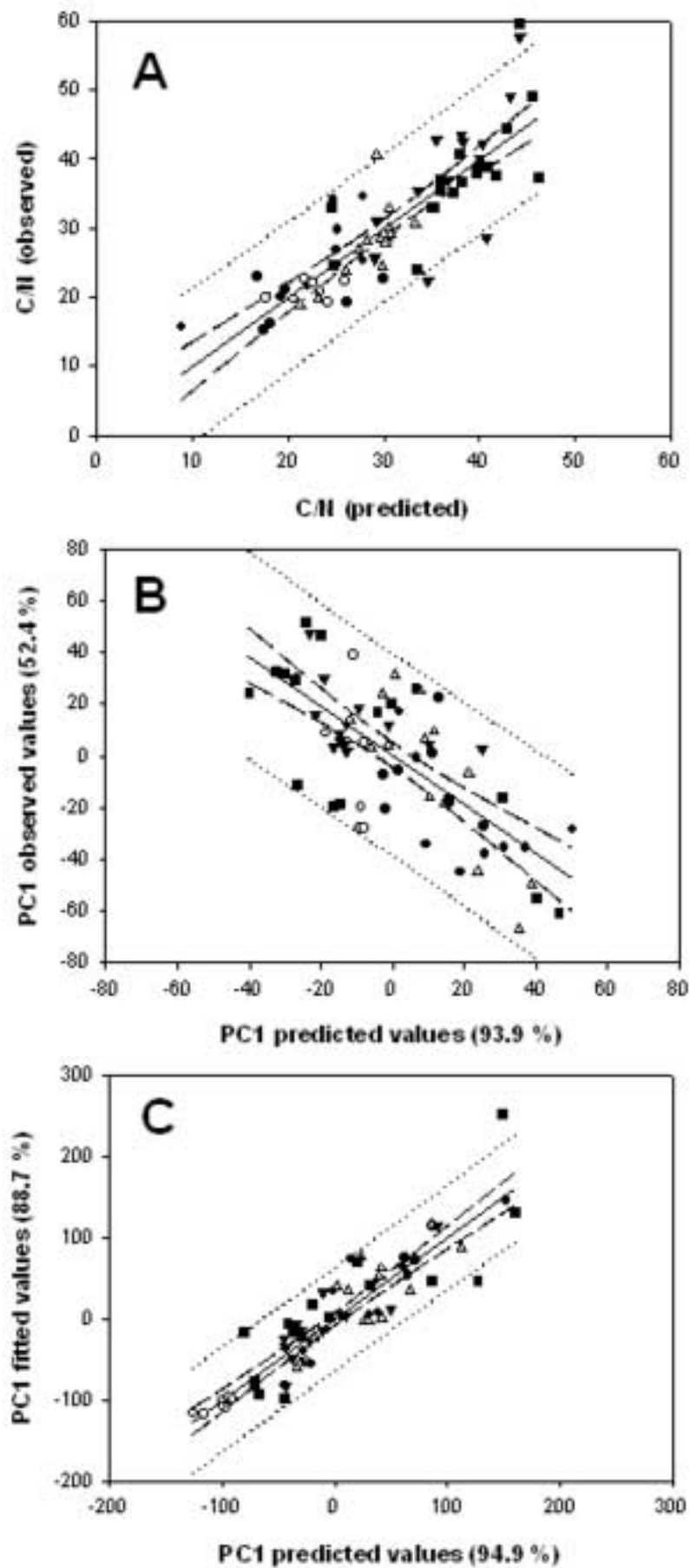


Table 1. Origin and general characteristics of peat samples

Country	Site	Regeneration stage ^a	Dominant vegetation ^b	Years since abandonment (estimate)
Finland (Aitoneva)	A	Early	<i>Eriophorum vaginatum</i>	10
	B	Early	<i>Eriophorum vaginatum</i>	10
	C	Early	<i>Carex rostrata</i>	10
	D*	Early	<i>Sphagnum fallax</i>	10
	E	Bare	-	
France (Bauppte)	A	Bare	-	5-10
	B	Early	<i>Eriophorum vaginatum</i>	5-10
France (Le Russey)	A	Bare	-	5
	B*	Early	<i>Sphagnum fallax</i> , <i>Eriophorum angustifolium</i>	5
	C*	Advanced	<i>Sphagnum fallax</i> , <i>Eriophorum angustifolium</i> , <i>Calluna vulgaris</i>	<50
	D	Reference	<i>Sphagnum fallax</i> , <i>Eriophorum angustifolium</i> , <i>Calluna vulgaris</i>	Intact
Switzerland (Chaux d'Abel)	A*	Early	<i>S. fallax</i> (discontinuous), <i>E. vaginatum</i> , <i>Polytrichum commune</i> , <i>P. strictum</i>	>25
	B	Intermediate	<i>S. fallax</i> , <i>E. vaginatum</i> , <i>Polytrichum commune</i> , <i>P. strictum</i>	>35
	C	Advanced	<i>S. fallax</i> (continuous), <i>E. vaginatum</i> , <i>Polytrichum commune</i> , <i>P. strictum</i> , <i>Vaccinium spp.</i>	40-45
	D*	Reference	<i>S. fallax</i> (continuous), <i>E. vaginatum</i> , <i>Polytrichum commune</i> , <i>P. strictum</i> , <i>Vaccinium spp.</i>	Intact
Scotland (Middlemuir)	A	Early	-	5
	B	Early	<i>E. vaginatum</i> , <i>Agrostis canina</i> , <i>Calluna vulgaris</i> , <i>E. angustifolium</i> , <i>S. auriculatum</i> , <i>S. cuspidatum</i>	5
	C	Early	<i>E. angustifolium</i> , <i>S. auriculatum</i> , <i>E. vaginatum</i> , <i>S. cuspidatum</i>	5
	D	Advanced	<i>S. palustre</i> , <i>C. vulgaris</i> , <i>E. vaginatum</i> , <i>Erica tetralix</i> , <i>Deschampsia flexuosa</i> , <i>Molinia caerulea</i>	50

^a Determined by assessment of vegetation diversity and depth of newly formed peat ^b Based on % cover estimates. Only vegetation with >10% cover reported * Horizon 3 samples not analysed.

Table 2. Assignment of the principal descriptive IR absorption bands in peat samples

Wavenumber, cm ⁻¹	Assignment	Characterisation	Reference
3340	γ (O-H) stretching	Cellulose, in samples with defined 3340 peak	Cocozza et al., 2003
2920	antisymmetric CH ₂	Fats, wax, lipids	Niemeyer et al., 1992; Cocozza et al., 2003
2850	symmetric CH ₂	Fats, wax, lipids	Niemeyer et al., 1992; Cocozza et al., 2003
1720	C=O stretch of COOH or COOR	Carboxylic acids, aromatic esters	Niemeyer et al., 1992; Haberhauer et al., 1998; Cocozza et al., 2003; Gondar et al., 2005
1710-1707	C=O stretch of COOH	Free organic acids	Gondar et al., 2005
1653	C=O of amide I	Proteinaceous origin	Ibarra et al., 1996; Zaccheo et al., 2002
1650-1600	Aromatic C=C stretching and/or asymmetric C-O stretch in COO-	Lignin and other aromatics, or aromatic or aliphatic carboxylates	Niemeyer et al., 1992; Cocozza et al., 2003
1550	N-H in plane (amide-II)	Proteinaceous origin	Ibarra et al., 1996; Zaccheo et al., 2002
1515-1513	Aromatic C=C stretching	Lignin/Phenolic backbone	Cocozza et al., 2003
1426	Symmetric C-O stretch from COO- or stretch and OH deformation (COOH)	Carboxylate/Carboxylic structures (humic acids)	Parker, 1971
1450, 1371	C-H deformations	Phenolic (lignin) and aliphatic structures	Parker, 1971
1265 (approximately)	C-O stretching of phenolic OH and/or arylmethylethers	Indicative of lignin backbone	Niemeyer et al., 1992; Ibarra et al., 1996
1080-1030	Combination of C-O stretching and O-H deformation	Polysaccharides	Grube et al., 2006
900	Out of phase ring stretching (ring 'breathing')	Cellulose, corresponding band to sharpened 3340 peak	Zaccheo et al., 2002
720	CH ₂ wag	Long chain (>C4) alkanes	Ibarra et al., 1996
835	Aromatic CH out of plane	Lignin	Zaccheo et al., 2002

Table 3. Organic matter parameters measured with average, standard deviation and range observed.

Parameter	Average	SD	Range
Elemental			
Total C (%)	52.5	4.0	42.9-60.6
Total N (%)	1.9	0.6	0.9-3.2
C/N ratio	30.6	9.9	15.1-59.7
Micromorphology			
Amorphous organic matter (%)	20.7	15.6	0.9-71.8
Preserved <i>Cyperaceae</i> (%)	9.6	19.0	0-79.8
Preserved <i>Sphagnum</i> (%)	4.6	6.9	0-27.3
Preserved <i>Polytrichum</i> (%)	1.1	3.9	0-22.1
Undetermined preserved tissue (%)	2.6	4.6	0-19.1
Structureless <i>Cyperaceae</i> (%)	4.5	9.4	0-41.8
Structureless <i>Sphagnum</i> (%)	0.5	1.3	0-5.2
Structureless <i>Polytrichum</i> (%)	0.1	1.0	0-8.1
Undetermined structureless (%)	10.9	9.9	0.2-43.6
Mucilage (%)	40.8	24.1	0-94.4
Microorganisms (%)	3.1	2.4	0.1-12.9
Cuticles/Spores/Pollen (%)	1.1	3.6	0-28.4
Gelified or oxidised debris (%)	0.1	0.4	0-2.8
Carbohydrates			
Total sugars (mg g ⁻¹)	134.9	60.2	40.6-346.5
Hemicellulosic sugars (mg g ⁻¹)	86.9	40.1	27.2-179.9
Cellulosic sugars (mg g ⁻¹)	47.9	28.2	10.7-173.2
Xylose (%)	19.4	4.1	10.5-31.0
Arabinose (%)	6.6	4.9	1.7-19.6
Hemicellulosic glucose (%)	38.2	11.3	16.4-58.5
Mannose (%)	10.4	1.8	6.3-16.4
Rhamnose (%)	7.5	1.8	2.7-12.6
Galactose (%)	6.4	6.5	0.2-26.9
Ribose (%)	2.0	1.8	0-6.3
Fucose (%)	9.5	6.2	1.8-23.2

Table 4. Partial least squares analysis results of zero-order FTIR spectra vs. peat micromorphological and chemical properties.

Parameter	No. of latent roots in univariate PLS (variance accounted for, r ² in %)	RMSECV ^a in univariate PLS	No. of latent roots in multivariate PLS (variance accounted for, r ² in %)
Elemental			
Total C (%)	6 (81.6) *** ^b	2.1	6 (75.6)
Total N (%)	6 (68.8) ***	0.4	6 (67.5)
C/N ratio	6 (70.6) ***	6.4	6 (70.4)
Micromorphology			
Amorphous organic matter (%)	1 (9.0) ***	15.2	2 (8.9)
Preserved <i>Cyperaceae</i> (%)	2 (51.0) ***	14.3	2 (50.4)
Preserved <i>Sphagnum</i> (%)	1 (8.0) ***	6.8	2 (7.7)
Preserved <i>Polytrichum</i> (%)	1 (19.3) ***	3.7	2 (22.9)
Undetermined preserved tissue (%)	1 (2.4) ^{ns}	4.7	2 (2.6)
Structureless <i>Cyperaceae</i> (%)	1 (16.5) ***	8.7	2 (16.4)
Structureless <i>Sphagnum</i> (%)	1 (9.2) **	1.3	2 (0.2)
Structureless <i>Polytrichum</i> (%)	1 (4.1) ^{ns}	1.0	2 (5.4)
Undetermined structureless (%)	1 (9.7) **	9.6	2 (6.4)
Mucilage (%)	2 (40.7) ***	19.7	2 (37.8)
Microorganisms (%)	1 (11.4) **	2.3	2 (11.7)
Cuticles/Spores/Pollen (%)	1 (10.9) ^{ns}	3.7	2 (10.7)
Gelified or oxidised debris (%)	1 (12.1) ***	0.4	2 (2.9)
Carbohydrates			
Total sugars (mg g ⁻¹)	4 (81.2) ***	29.5	4 (80.7)
Hemicellulosic sugars (mg g ⁻¹)	4 (83.5) ***	17.7	4 (82.9)
Cellulosic sugars (mg g ⁻¹)	2 (43.8) ***	22.2	4 (46.9)
Xylose (%)	3 (41.2) ***	3.4	4 (36.9)
Arabinose (%)	2 (45.7) ***	3.8	4 (41.4)
Hemicellulosic glucose (%)	4 (60.1) ***	7.8	4 (47.8)
Mannose (%)	3 (17.7) ***	1.8	4 (8.2)
Rhamnose (%)	4 (46.3) ***	1.6	4 (21.0)
Galactose (%)	2 (59.3) ***	4.3	4 (58.0)
Ribose (%)	4 (64.0) ***	1.2	4 (57.5)
Fucose (%)	4 (84.9) ***	2.8	4 (81.8)

^a Root mean square error of cross-validation in univariate PLS. ^b Significance at $p < 0.05$ -*, $p < 0.01$ - **, $p < 0.001$ - ***, ns - not significant.